Eur. Phys. J. A **1**, 77–83 (1998)

THE EUROPEAN PHYSICAL JOURNAL A

Critical behaviour in Au fragmentation at 10.7A GeV

M.I. Adamovich[14], M.M. Aggarwal[4], Y.A. Alexandrov[14], R. Amirikas[18], N.P. Andreeva[1], F.A. Avetyan[22],S.K. Badyal[8], A.M. Bakich[18], E.S. Basova[19], K.B. Bhalla[7], A. Bhasin[8], V.S. Bhatia[4], V.G. Bogdanov[15], V. Bradnova[6], V.I. Bubnov[1], X. Cai[21], I.Y. Chasnikov[1], G.M. Chen[2], L.P. Chernova[20], M.M. Chernyavski[14], S. Dhamija[4], A.S. Gaitinov[1], E.R. Ganssauge[13], S. Garpman[12], S.G. Gerassimov[14], J. Grote[16], K.G. Gulamov[20], S.K. Gupta[7], V.K. Gupta[8], M. Haiduc[3], U. Henjes[13], B. Jakobsson[12], L. Just[10], E.K. Kanygina[1], M. Karabova[9], L. Karlsson[12], S.P. Kharlamov[14], A.D. Kovalenko[6], S.A. Krasnov[6], V. Kumar[7], V.G. Larionova[14], Y.X. Li[5], L.S. Liu[21], Z.G. Liu[5], S. Lokanathan[7], J.J. Lord[16], N.S. Lukicheva[20], Y. Lu[2], S.B. Luo[11], L.K. Mangotra[8], I. Manhas[8], N.A. Marutyan[22], A.K. Musaeva[1], S.Z. Nasyrov[19], V.S. Navotny[20], J. Nystrand[12], G.I. Orlova[14], I. Otterlund[12], L.S. Peak[18], N.G. Peresadko[14], V.A. Plyushchev[15], W.Y. Qian[21], Y.M. Qin[11], R. Raniwala[7], N.K. Rao[8], J-T. Rhee[17], M. Roeper[13], V.V. Rusakova[6], N. Saidkhanov[20], N.A. Salmanova[14], L.G. Sarkisova[22], V.R. Sarkisyan[22], A.M. Seitimbetov[1], R. Sethi[4], C.I. Shakhova[1], B. Singh[7], D. Skelding[16], K. Söderström[12], E. Stenlund[12], L.N. Svechnikova[20], N.A. Tawfik[13], M. Tothova[9], M.I. Tretyakova[14], T.P. Trofimova[19], U.I. Tuleeva[19], S. Vokal[9], J. Vrlakova[9], H.Q. Wang[12,21], S.H. Wang[2], X.R. Wang[21], Z.Q. Weng[5], R.J. Wilkes[16], C.B. Yang[21], D.H. Zhang[11], P.Y. Zheng[2], S.I. Zhokhova[20], D.C. Zhou[21], EMU01-Collaboration

[1] High Energy Physics Institute, Almaty, Kazakstan
[2] Institute of High Energy Physics, Academia Sinica, Beijing, China
[3] Institute for Gravitation and Space Research, Bucharest, Romania
[4] Department of Physics, Panjab University, Chandigarh, India
[5] Department of Physics, Hunan Education Institute, Changsha, Hunan, China
[6] Laboratory of High Energies, Joint Institute for Nuclear Research (JINR), Dubna, Russia
[7] Department of Physics, University of Rajasthan, Jaipur, India
[8] Department of Physics, University of Jammu, Jammu, India
[9] Department of Nuclear Physics and Biophysics, Safarik University, Kosice, Slovakia
[10] Institute of Experimental Physics, Slovak Academy of Sciences, Kosice, Slovakia
[11] Department of Physics, Shanxi Normal University, Linfen, Shanxi, China
[12] Department of Physics, University of Lund, Lund, Sweden
[13] F.B. Physik, Philipps University, Marburg, Germany
[14] Lab. of Cosmic Physics, P.N. Lebedev Institute of Physics, Moscow, Russia
[15] V.G. Khlopin Radium Institute, St. Petersburg, Russia
[16] Department of Physics, University of Washington, Seattle, Washington, USA
[17] Department of Physics, Kon-Kuk University, Seoul, Korea
[18] School of Physics, University of Sydney, Sydney, Australia
[19] Lab. of Relativistic Nuclear Physics, Institute of Nuclear Physics, Tashkent, Uzbekistan
[20] Lab. of High Energies, Physical-Technical Institute, Tashkent, Uzbekistan
[21] Institute of Particle Physics, Hua-Zhong Normal University, Wuhan, Hubei, China
[22] Yerevan Physics Institute, Yerevan, Armenia

Received: 23 September 1997

Abstract. The complete charge distribution of products from Au nuclei fragmenting in nuclear emulsion at 10.7A GeV has been measured. Multiplicities of produced particles and particles associated with the target source are used to select peripheral and central events. A statistical analysis, based on event-by-event charge distributions, show that a population of subcritical, critical and supercritical events, i.e. a phase transition like behaviour, is observed among peripheral collisions.

PACS. 25.75.-q Relativistic heavy-ion collisions

1 Introduction

The observation of multifragmentation in both p-nucleus [1,2] and nucleus-nucleus reactions [3-9] is well established through experiments utilizing different techniques. In fact it appears as if a nucleus, excited to high enough energy, breaks into pieces with a size (or charge) distribution given by statistical (microcanonical) formalism independent of

the dynamical prehistory. Therefore it does not appear to be necessary that the reaction proceeds through a compression/decompression evolution to bring it into a mechanical instable phase. Fragment size data alone cannot tell whether multifragmentation reactions exhibit a thermodynamic behaviour, with a liquid-gas phase transition, or just a statistically determined breakup, e.g. of percolation type [10], which still may simulate a transition [11].

In order to investigate the critical behaviour in a collision sample it has been suggested to correlate various parameters based on the event-by-event mass or charge distribution of the source that breaks up [12]. In counter detector data, this kind of analysis is often severely restricted by the detector acceptance in space and phase-space although the most recent 4π detector systems have overcome this difficulty to some extent [13,14]. The electron sensitive nuclear emulsion stack, which is used in this investigation, is a detector with nearly no space or phase-space restrictions for charged fragments and it has been used in a few experiments on criticality before [15,16].

It has however been argued that in emulsion experiments the mixture between emission sources, both with respect to origin and size, is a severe shortcoming for collisions at a few hundreds of MeV/nucleon or even at a few GeV/nucleon. At 10.7A GeV it is reasonably easy to make a strict separation between fragments from different sources because of the large rapidity gap between the projectile and target source (3.21 units). Au induced collisions of peripheral nature and collisions with light emulsion nuclei (H,C,N,O) do all create an initial source close in size to the Au nucleus whereas central (Br,Ag) collisions create on the average slightly larger, and more excited, participant sources. A straight line geometry estimate gives in fact $< A_{part} > = 235$ for central (b= 0-3 fm) Au + Ag,Br collisions. Both kinds of fragmenting sources are investigated in this paper. The ionization measurement methods do allow us to measure the complete Z distribution. Combining this with the excellent spatial resolution of the emulsion detector provides data on critical behaviour which should stand on solid ground.

2 Experimental details

Several stacks of electron sensitive, NIKFI BR-2 emulsions, exposed horizontally to the 10.7 A GeV Au beam from the BNL synchrotron (experiment BNL E863) have been scanned along-the-track. 1681 minimum bias events have been investigated with respect to Au breakup.

Selection of projectile-associated fragments(PF) with charge ($Z_{PF} \geq 2$) has been made from the requirements, i) that the emission angle should be less than 52 mr corresponding to 3σ (three standard deviations of the transverse momentum) in the groundstate Fermi distribution of Au and ii) that the ionization remains constant over 1 cm from the collision point. In rare cases the latter criterion is impossible to control (secondary collisions etc.) and therefore also the requirement that $\Sigma\ Z_{PF} \leq 79$ is introduced. The angles are determined by measuring the coordinates of two points on the primary and secondary tracks separated by 10 mm, if possible. Furthermore the number of shower particles, N_s (projectile protons and pions with E > 60 MeV) and the number of black- (target associated particles, protons with E < 36 MeV) and grey (essentially knock-out protons with 36 < E < 400 MeV) prong producing particles have been registered. The number of produced pions, N_π, is estimated as,

$$N_\pi = N_s - (79 - \sum Z_{PF}). \quad (1)$$

The charge, Z_{PF}, has been determined from CCD profile measurements, from delta ray + gap counting and from optical photometric width measurements + gap counting. Each method is used for about 1/3 of the events. In the CCD photometer measurements, described in [17], the FW2/3M of the absorption profile was determined for a length of 2 mm divided into 200 windows at a position of the track that is free from disturbing background tracks. Different slit widths from 2.5 to 8.0 μm are used for different Z regions in order to optimize the resolution. The Z calibration was performed with the help of beam (Z = 79), fission-like (events that contain only two fragments) and Z = 1 - 8 tracks, safely identified by gap counting. A typical result for one scanner (individual calibration is used) is shown in Fig. 1a which actually also includes some tracks with other charges determined independently by filar micrometer width measurements.

In the second set of events, light fragment tracks, estimated to have Z = 2 - 7, were identifed by counting the number of gaps (N_{ga}) with a length, $\ell > 1$, > 1.5 and > 2 μm. In this charge region it is fairly simple to collect enough safely identified tracks and obtain calibration functions,

$$Z = a - b \cdot N^c. \quad (2)$$

Here $N = N_{ga} \cdot < N_\alpha > / N_\alpha$, where $< N_\alpha >$ is the average number of gaps on alpha particle tracks and N_α the number of gaps on an alpha particle track from the same or a close collisions with dip angle as close as possible to the measured fragment. The parameters a, b and c are determined individually for $\ell > 1$, 1.5 and 2 μm ([61.9, 55.0, 0.023], [11.3, 6.0, 0.188], [6.9, 3.2, 0.606]). Whenever the Z determination differs between these three equations the proper average Z is chosen. In the charge region Z=7 - 79 tracks were identifed by delta-ray counting. Three different lengths, ℓ (of delta rays) were chosen and the calibration equations are of the form,

$$Z = d + e \cdot N \quad (3)$$

where $N = N_d \cdot < N_{proj} > / N_{proj}$ and N_d is the number of delta-rays on the track we identify, N_{proj} the number of a delta-rays on the projectile from this collision and $< N_{proj} >$ the average number of delta-rays on all projectiles. The parameters d and e are determined to [6.0, 0.13] for Z = 7 - 15 (δ rays with $\ell > 2$ μm), [6.0, 0.46] for Z = 15 - 50 (δ rays with $\ell > 7.5$ μm) and [30.0, 0.65] for Z = 40 - 79 (δ rays with $\ell > 15$ μm). When overlapping calibration exists the average value is chosen. The calibration is performed via,

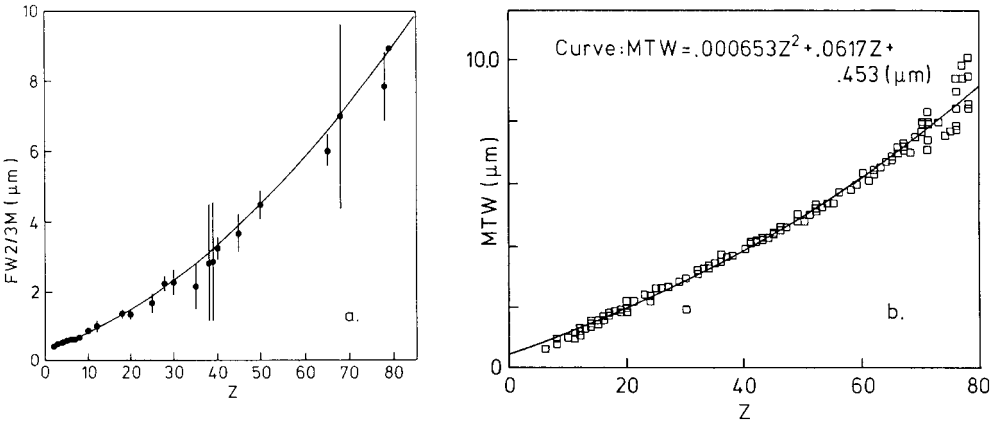

Fig. 1. a Charge vs. track width calibration curve in the Lund CCD profile photometer. **b** charge vs. track width distribution from the Moscow CADIM profile photometer [18]

1) electromagnetic dissociation (ED) events,
2) events with a number of produced particles ≤ 5 and
3) events with more than four Z>2 fragments where gap counting on Z = 1,2,3,4 fragments is enough to allow a good estimation of one (eventual) remaining heavier fragment.

In the third set of data the charge of the light fragments was also determined by gap counting ($2 \leq Z \leq 6$) and delta ray counting ($4 \leq Z \leq 18$) but in addition the charge of the heavy fragments ($Z \geq 10$) was determined by an optical profile photometer (CADIM station [18]). The width is in this case integrated over a length of 1.4 - 2.8 mm divided into 40 - 60 windows. Again the calibration is performed with the help of beam tracks, fission tracks and light tracks where gap- and delta ray counting give a safe result. Figure 1b shows the MTW(mean track width) distribution for this part of the material.

The result of the complete Z distributions determined by the three methods are compared in Fig. 2b. Only the Z=79 channel exhibits a significant difference. This should however hardly be interpreted as differences in the charge measurement methods but rather as a difference in the scanning efficiency, either for the most peripheral (smallest multiplicity) events or for projectile proton tracks (shower particles) in peripheral collisions.

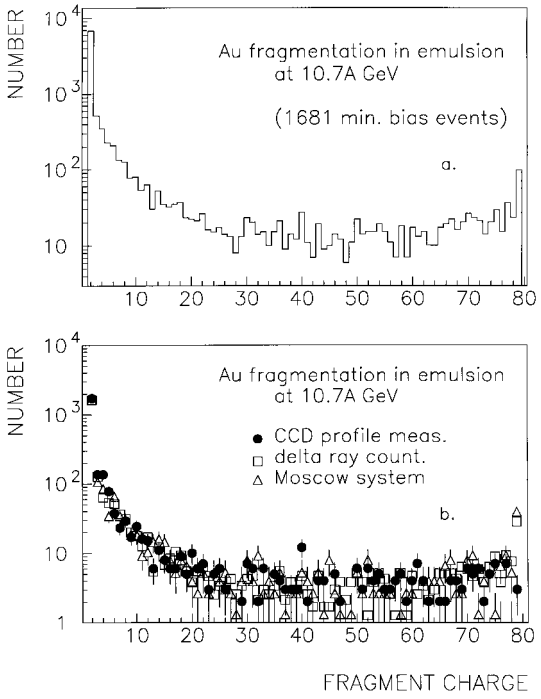

Fig. 2. a Au fragmentation charge distribution in the total sample. **b** Fragmentation distributions measured by the Lund CCD profile photometer [17], by delta ray counting and by the Moscow profile photometer [18]

3 Experimental results

3.1 Charge distributions

The above mentioned difference in yield of the Au (Z = 79) fragments, between the samples representing different measurement methods, is of little importance for the further analysis and therefore all samples are added to a total minimum bias sample as in Fig. 2a. The charge distribution exhibits the expected U-shape. It should be noticed that the number of hydrogen fragments, which is left out in the figure, is estimated to 49277 from charge conservation (or more correctly 50200 if the nucleon net charge exchange from the isospin weights of π^+, π^- and π^o production is considered). Both hydrogen- and helium fragments thus stick out from the general form of the distribution in the sense that they are substantially more frequent. This is not surprising, since pre-equilibrium processes, e.g. directly knocked out protons and alpha particles, are expected in addition to "normal" statistical emission.

The Z_{bound} parameter, introduced in the ALADIN spectrometer data [19], cannot be used directly for independent impact parameter selection because it is directly correlated to the event-by-event charge distribution. The same is to some extent true for the multiplicity of shower particles (N_s). The pion multiplicity is a better parameter. A rough estimate of the number of charged pions is given by (1).

In Fig. 3a the charge distributions in events biased by a strong cut in N_s or N_π are explored. In both cases about 25% of the total number of events remain. Some

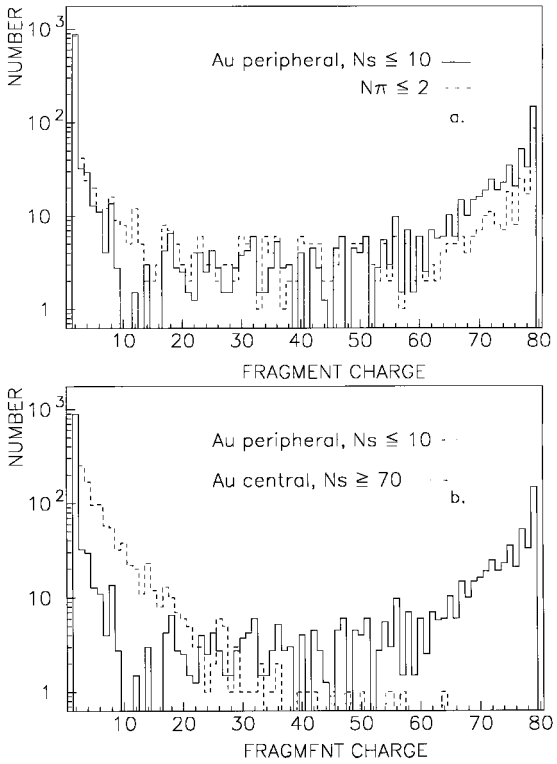

Fig. 3. a Au fragmentation charge distribution in a: peripheral collisions selected by N_s (*solid histogram*) and N_π (*dashed histogram*) criteria and **b** peripheral (*solid*) and central (*dashed*) collisions selected by N_s criteria

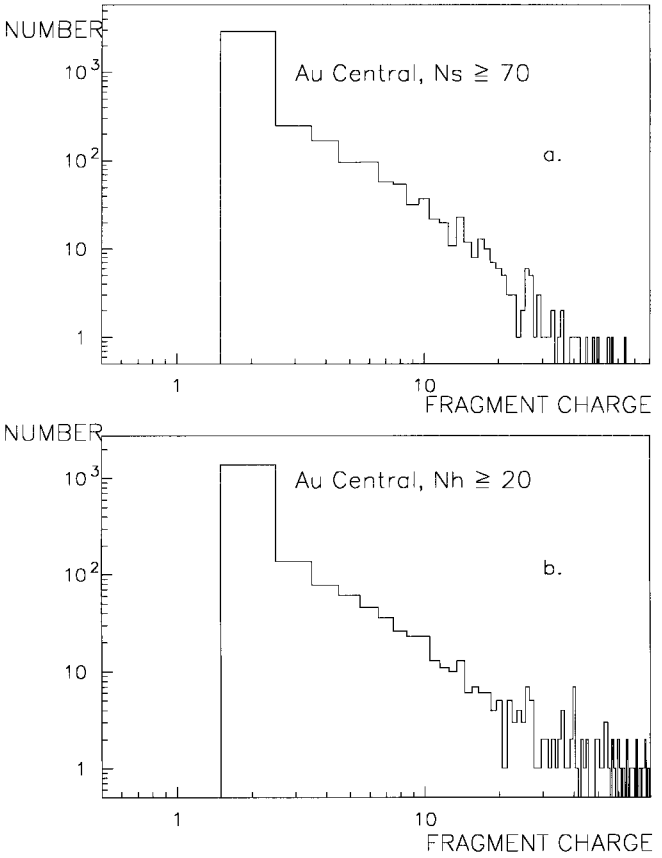

Fig. 4. a Au fragmentation charge distribution in central collisions selected **a** by the $N_s \geq 70$ criterion and **b** by the $N_h \geq 20$ criterion

tendency of a smaller fraction of heavy fragments with the N_s restriction appears but since the difference is marginal we use subsequently the directly measured N_s parameter for the impact parameter selection. Figure 3b presents a comparison between central events selected by a very high N_s cut and peripheral events selected by the same $N_s \leq 10$ cut as above. The absence of heavy fragments in the former sample is obvious and shows that the excitation energy is on the average much higher. A proper high N_π cut shows very much the same behaviour.

The multiplicity of heavy prong (black + grey) producing particles (N_h) is a parameter which is not biased by the projectile fragment charge distribution. The mixed target is of course a complication which introduces a mixture of peripheral and central collisions with light emulsion nuclei (H, C, N, O) and peripheral collisions with heavy emulsion nuclei (Br, Ag) for events with a small N_h. More important is however that the Au projectile should be weakly excited in all these events compared to central Au + Br,Ag collisions.

In Fig. 4 we compare the central samples ($\sim$ 25%) selected by N_s and N_h criteria. The Z distributions follow a power law,

$$N_{PF}(Z) = C \cdot Z^{-\tau} \qquad (4)$$

over the whole Z region except for Z = 1 (not shown in Fig. 4) and Z = 2. The values of τ are 2.20 and 2.39 respectively (see Table 1) which should be compared to the expected $\tau = 7/3$ for a second order liquid-gas phase transition [20]. It should be pointed out that if there are channels which contain zero fragments, they are given the weight 0.1 instead of $\sqrt{N} = 0$. The power law is a necessary condition for a phase transition but it does not prove the existence of this transition. It has been pointed out [21] that unless a strict impact parameter selection is made, it may well happen that adding up a number of binomial Z distributions for different impact parameter samples also creates an exponential distribution with a similar τ value as given by the phase transition.

Table 1 further explores the τ paramater in different event samples. Obviously the power law is only valid in a limited Z region for the peripheral samples (Fig. 3b) which is a natural consequence of the heavy fragment which almost always remains in such collisions. The choice of the upper Z limit is delicate and in Table 1 all fits to peripheral event distributions are made in the $3 \leq Z \leq 15$ region. Anyway these distributions appear to be less steep than the central event distributions except when restricting the upper N_s limit very strongly. On the other hand it appears as if the central samples do give τ values close to those expected for a system that explores a critical behaviour. The tendency of getting closer to the "critical" $\tau \sim 2.2$ - 2.4 region with increasing degree of centrality is significant.

Table 1. The critical exponent τ from calculations and experimental Au fragmentation data with various triggers for centrality (and peripherality)

Type of calculation/event	τ parameter	χ^2/d.o.f.
Liquid-gas scenario	7/3	-
Site percolation	2.20±0.05	-
Central events		
Au fragmentation, $N_s \geq 50$	1.83± 0.03	1.18
Au fragmentation, $N_s \geq 70$		
$3 \leq Z \leq 40$	2.12± 0.04	1.93
$3 \leq Z \leq 79$	2.22± 0.04	1.18
Au fragmentation, $N_h \geq 20$	2.39± 0.05	2.07
Peripheral events		
Au fragmentation, $N_s \leq 10$	2.72± 0.22	1.49
Au fragmentation, $N_s \leq 20$	1.83± 0.10	1.18
Au fragmentation, $N_\pi \leq 2$	1.55± 0.14	1.08
Au fragmentation, $N_h \leq 2$	1.82± 0.07	2.29

3.2 Correlations between critical parameters

In the search for critical behaviour one often uses the moments of the size or charge distribution as suggested by X. Campi [12] several years ago. The k:th moment of event i is normalized by the first moment,

$$S_i^k = \sum_{Z=1}^{79} Z^k n_i(Z) / [\sum_{Z=1}^{79} Z n_i(Z)] \qquad (5)$$

where $n_i(Z)$ is the number of fragments with charge Z. For a finite system, like the gold nucleus with 79 charge units, the choice of partitions is certainly finite. Therefore correlations of the type, ln Z_{max} - ln S_k, have strong mathematical restrictions and these are even strengthened by excluding the heaviest fragment when calculating the k:th moment. This is the reason for the triangular shape in Fig. 5 a which shows the experimental ln Z_{max} - ln S_2 correlation for all (minimum bias) events. In Fig. 5 b the mathematical restrictions are shown and indeed the minimum bias events are scattered all over the available area which is a signature for a large dispersion both in excitation and effective source size.

In order to select events with more limited excitation of sources with a quite narrow size distribution around Z=79 we choose first the strong $N_s \leq 10$ cut in Fig. 5c. The selection of events in ln Z_{max} - ln S_k space is dramatic. The supercritical (lower) band and the subcritical (upper) band are now clearly visible and the asymptotic behaviour, limited by the finite size restriction in ln S_2 to 3.68, is obvious with several events in the transitional region. These events appears as fission-like, although they have little in common with classical fission. The extreme central events, as selected by high N_s (or pion) multiplicity (Fig. 5e), are almost complementary to the critical sample. They certainly populate a large part of the available space but avoid the subcritical and the critical regions. Possibly the excitation is too high and too widely distributed in this case to allow for a critical behaviour.

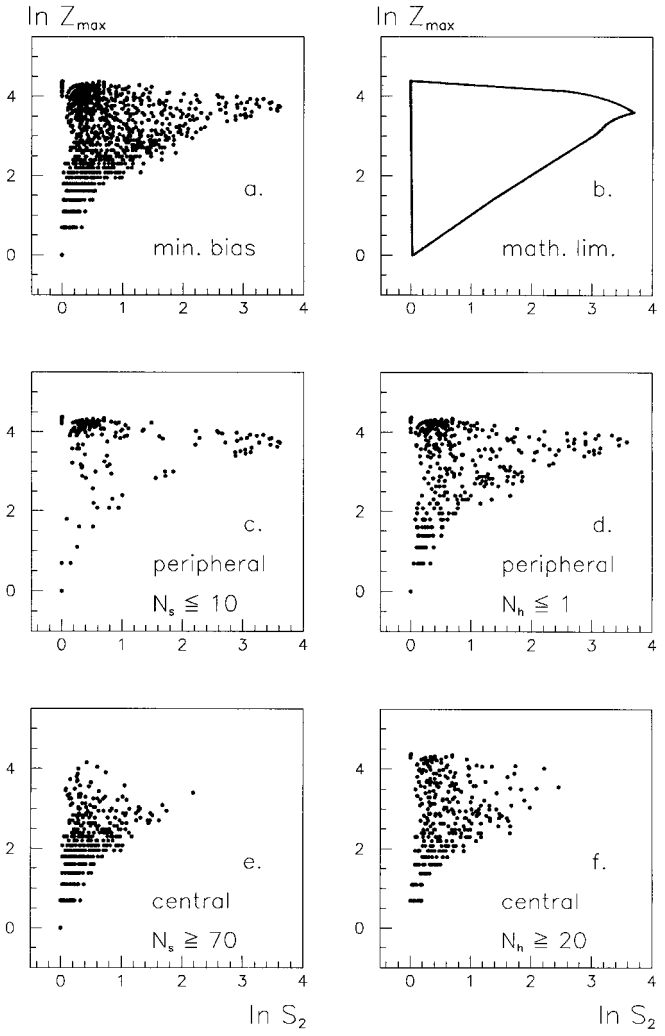

Fig. 5. ln Z_{max} - ln S_2 correlations for Au fragmentation charge distribution in **a** the total minimum bias sample, **b** the mathematical limits, **c** a peripheral $N_s \leq 10$ sample, **d** a peripheral $N_h \leq 1$ sample, **e** a central $N_s \geq 70$ sample and **f** a central $N_h \geq 20$ sample

The other parameter for peripheral events, $N_h \leq 1$, which normally is believed to pick out H events, peripheral CNO events and very peripheral AgBr events does not show the same strong selectivity for critical collisions (Fig. 5d), whereas the central, $N_h \geq 20$, AgBr sample (Fig. 5f) shows much the same behaviour as the central sample based on the N_s selection. It should be noticed that investigations in high energy emulsion collisions do show that the $< N_h >$ - N_s or the $< N_h >$ - impact parameter correlation is not straightforward and that a low N_h cut actually may select both very peripheral and very central collisions. The complicated relation between the black or grey prong constituents of N_h and N_s is discussed in [22].

In [12] the expected behaviour of the relative variance, γ_2, when plotted against the reduced multiplicity, n, is shown for statistical models that should contain a critical

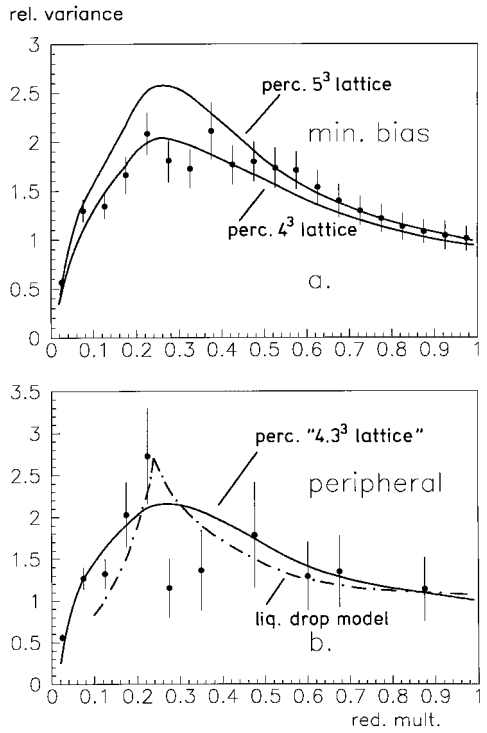

Fig. 6. γ_2 versus the reduced multiplicity, n for Au fragmentation in **a** all events and **b** peripheral events selected by the $N_s \leq 10$ criterion. All *solid curves* refer to standard 3-d bond percolation calculations. The *dot-dashed curve* comes from a liquid drop model calculation [23]

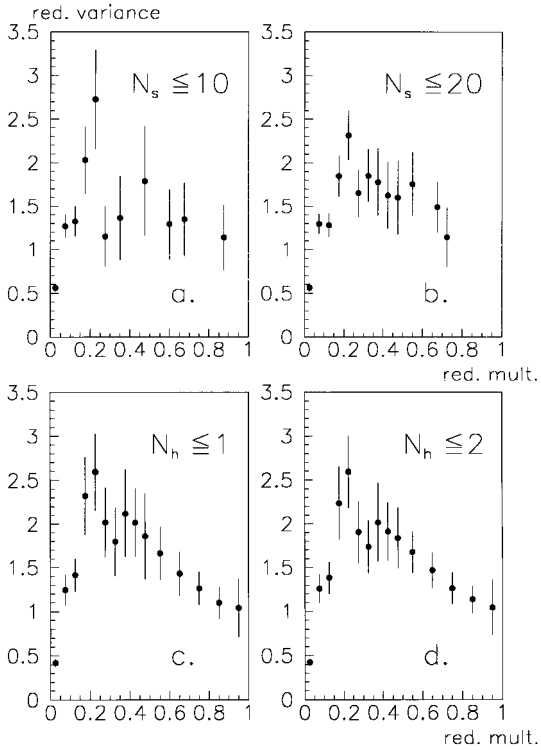

Fig. 7. γ_2 versus the reduced multiplicity, n for Au fragmentation in various samples of events, **a** $N_s \leq 10$, **b** $N_s \leq 20$, **c** $N_h \leq 1$ and **d** $N_h \leq 2$

behaviour. The variance, V is related to γ_2 through,

$$\gamma_2 = \frac{p_2 \cdot p_o}{p_1^2} = \frac{V}{< Z >^2} + 1$$
$$p_k = \sum_Z Z^k n_i(Z)/79$$

where 79 comes from the assumption that all sources originally contain 79 charges. A clear maximum at the critical point, even for a rather small system, should remain from the asymptotic behaviour of an infinite system. We show in Fig. 6a that the minimum bias sample of Au fragmentation behaves very much as expected for a standard 3-d percolation with a lattice size between 4^3 and 5^3 . When selecting the most peripheral events by means of the $N_s \leq 10$ cut (Fig. 6b) we see that the pure percolation behaviour is not applicable in the critical n-region around n = 0.22.

Instead a combination of a statistical multifragmentation process and an evaporation chain for cooling the preexcited fragments is introduced as in the Copenhagen model [23]. There the liquid-drop formalism is used to separate matter into a gaseous and a liquid phase. We do observe a better agreement with data for the peripheral events in the critical region as shown in Fig. 6b. Actually it appears as if the data show a stronger phase-transition behaviour. The statistics in this sample is not overwhelming, 439 events, but if the complete behaviour in the critical region, say from n = 0.15 to n = 0.4 is considered there is a significance in this statement. Thus the delicate requirement of peripheral events may create a sample of fragmenting sources which is quite homogeneous in size and excitation energy.

In Fig. 7 we show the γ_2 - n behaviour also for other peripheral event samples. Although the peak remains in the n = 0.2 - 0.25 interval in all cases it is obvious that a less stringent N_s cut or the choice of N_h as selecting parameter make the behaviour look more like what is expected from site percolation.

4 Conclusions

We have observed the expected U-shaped charge distribution in the breakup of Au nuclei in collisions with emulsion nuclei at 10.7A GeV. The $N \sim Z^\tau$ power law is however not very selective and the value of τ depends strongly on the Z interval for the fit.

The correlation between the largest fragment and the second moment of the charge distribution as well as the relative variance versus reduced multiplicity show a clear tendency for a critical behaviour when peripheral events are selected by a strong shower particle (or pion) multiplicity cut. The corresponding central event sample does not show this behaviour which indicates the difficulty in selecting events with the same size and excitation energy in this case. Using the heavy prong multiplicity for selecting peripheral events also does not show the same clear

evidence for critical behaviour as the N_s selected events. The expected asymptotic behaviour for a reduced multiplicity of 0.22±0.02, is weakened to a local maximum in the relative variance due to the finite size of the system. The peak height is well in agreement with a liquid drop prescription of the phase mixture.

The financial support from the Swedish Natural Science Research Council, the Australian Research Council, the German Federal Minister of Research and Technology, the Department of Science and Technology of India, the National Science Foundation of China, the Distinghuished Teacher Foundation the State Education Commission of China, the Fok Ying Tung Education, the RFBR grant 94-02-04220, the Grant Agency for Science at the Ministry of Education of Slovak Republic, the Slovak Academy of Sciences and the United States Department of energy and National Science Foundation is gratefully acknowledged.

References

1. P.A. Gorichev, O.V. Lozhkin, N.A. Perfilov and Yu. P. Yakovlev Sov. Phys. JETP **41**, 327 (1961)
2. J.E. Finn et al., Phys. Rev. Lett. **49**, 1321 (1982)
3. B. Jakobsson, G.Jönsson, B. Lindkvist and A. Oskarsson, Z. Physik **A307**, 293 (1982)
4. C.J. Waddington and P.S. Freier, Phys. Rev. **C31**, 888 (1985)
5. J.W. Harris et al., Nucl. Phys. **A471**, 241 (1987)
6. B. Jakobsson et al., Nucl. Phys. **A509**, 195 (1990)
7. C.A. Ogilvie et al., Phys. Rev. Lett. **67**, 1214 (1991)
8. R.T. de Souza et al., Phys. Lett. **B268**, 6 (1991)
9. G. Rusch, W. Heinrich, B. Wiegel, E. Winkel and J. Dreute, Phys. Rev. **C49**, 901 (1994)
10. D. Stauffer, Introduction to Percolation Theory, Taylor and Francis, London, 1985
11. D.H.E. Gross, Rep. Prog. Phys. **53**, 605 (1990)
12. X. Campi, J. Phys. Math. Gen. **19**, 917 (1986) and Phys. Lett. **208B**, 351 (1988)
13. J. Hubele et al., Z. Physik **A340**, 263 (1991)
14. J. Pouthas et al., Nucl. Instr. and Meth. **A357**, 418 (1995)
15. B. Jakobsson et al., Nucl. Phys. **A509**, 195 (1990)
16. M.L. Cherry et al., Phys. Rev. **C52**, 2652 (1995)
17. S. Angius, R. Elmér, B. Jakobsson, L. Karlsson and K. Söderström, Nucl. Instr. and Meth. **B63**, 359 (1992)
18. F. Bal, S. Tentindo and G. Vanderhaeghe, Nucl. Instr. and Meth. **225**, 661(1984)
19. C.A. Ogilvie et al., Phys Rev. Lett. **67**, 1214 (1991)
20. A.L. Goodman, J.I. Kapusta and A.M. Mekjian, Phys. Rev. **C30**, 851(1984)
21. W. Bauer, Report at the Int. Workshop on Phase Transitions in Nuclear Collisions, Copenhagen, Nov. 27-30, 1996, unpublished.
22. M.I. Adamovich et al., Z. Physik. **C65**, 429 (1995)
23. J.P. Bondorf et al., Nucl. Phys. **A443**, 321 (1985) and **A444**, 460 (1985)